

## Traveling-Wave States in Deep-Groove Directional Solidification

J. T. Gleeson,<sup>(1),(2)</sup> P. L. Finn,<sup>(1)</sup> and P. E. Cladis<sup>(1)</sup>

<sup>(1)</sup>*AT&T Bell Laboratories, Murray Hill, New Jersey 07974*

<sup>(2)</sup>*Department of Physics, Kent State University, Kent, Ohio 44242*

(Received 16 July 1990)

We observe asymmetric cells with deep grooves in directional solidification of a nearly pure material. These cells propagate laterally in direction determined by the sign of their asymmetry. Measurements of their phase speed and asymmetry agree qualitatively with current theories. We observe spatiotemporal dislocations and identify them with either lateral boundaries or crystal grain boundaries. At higher solidification speeds, we also observe periodic shape oscillations coherent over many cells.

PACS numbers: 81.30.Fb, 05.70.Ln, 61.50.Cj

Recently, there have been reports of exciting dynamical behavior in one-dimensional pattern-forming systems such as directional growth of both liquid crystals<sup>1,2</sup> and lamellar eutectics,<sup>3</sup> as well as directional viscous fingering.<sup>4</sup> In addition, there are new theories to describe this behavior.<sup>5,6</sup> In these systems, traveling waves (TW) composed of asymmetric cells are superimposed on a stationary one-dimensional periodic pattern of reflection-symmetric cells. Also characteristic of this behavior is the presence of spatiotemporal dislocations: sources and sinks in the pattern's phase. In contrast to previous observations<sup>1,3</sup> of localized inclusions of TW states,<sup>7</sup> we report here the first observation of steady-state traveling waves and corresponding asymmetric cells with deep grooves over the entire pattern. This behavior requires sustained phase sources and sinks that we also observe. We present evidence that sinks are related to the liquid-glass-solid contact angle at the lateral edges of the cellular array and the source is near a grain boundary in the original seed crystal. In addition, we measure both the phase speed of the traveling state and the asymmetry of the individual cells and find qualitative agreement with predictions.<sup>5</sup>

Coulet, Goldstein, and Gunaratne<sup>5</sup> argue that a one-dimensional stationary periodic pattern where the individual repeat units have reflection symmetry (even parity) may undergo a subcritical bifurcation to a dynamical parity-broken state.<sup>8</sup> The time dependence arises because asymmetric cells propagate along the direction of periodicity ( $x$ ) with a phase speed  $v_\phi$  proportional to their asymmetry  $A$ ; thus asymmetry dictates the direction of motion (or vice versa). They also attribute spatiotemporal dislocations to "kinks" in  $A(x)$ , where large phase gradients force the amplitude of the underlying symmetric pattern to zero. Independently, Levine, Rappel, and Riecke<sup>6</sup> find that if the undistorted state is unstable to perturbations of wave number  $q$  as well as  $2q$ , there exist asymmetric TW states where again asymmetry dictates the propagation direction.

We studied the interface between the liquid and solid phases of succinonitrile, purified by sublimation and condensation onto a cold finger. While the amount and nature of the remaining impurity is not known, the width of

the two-phase region is 4.0 K.<sup>9</sup> The purified material is vacuum loaded into  $0.10 \times 1.0 \times 50$ -mm rectangular glass capillaries that are then sealed at both ends. The succinonitrile, loaded as a liquid, is allowed to freeze freely when the capillary is removed from the vacuum oven, resulting in a multigrain crystal. In these experiments, we do not remove grain boundaries<sup>10</sup> from the seed crystal from which directional solidification begins. The capillary is then sandwiched between two glass cover slips and a thin layer of microscope immersion oil is introduced between the capillary and the cover slips to enhance heat transport and enable observation of the liquid-solid-glass contact point.

The loaded capillary is placed in an automated, high-resolution directional solidification stage.<sup>11</sup> In this apparatus, a temperature gradient  $G$  (70 K/cm) is created along the capillary axis by placing it across two temperature-regulated surfaces separated by a 4-mm air gap. The temperatures are chosen so that the solid-liquid interface lies in the gap and the desired temperature gradient is realized. The material is solidified by pulling the capillary at speed  $v$ , antiparallel to  $G$ . The whole apparatus is mounted on the stage of a microscope so that the solid-liquid interface may be directly viewed as well as recorded on videotape for later analysis. Simultaneously, one video line, perpendicular to the pulling direction and intersecting cell grooves, is digitized at fixed intervals, and then replotted sequentially to give an " $x-t$ " picture of the pattern's evolution (Fig. 1).

When the pulling speed exceeds a critical value  $v_c$  ( $\approx 2.0 \mu\text{m/s}$ ), the planar interface undergoes a morphological transition to an array of cells separated by deep grooves of liquid (Fig. 2). Since we never observe steady-state small-amplitude cells, this transition is likely an inverted bifurcation. Furthermore, the cellular instability nucleates and grows from crystal grain boundaries that intersect the interface. This also indicates an inverted bifurcation. In addition, there are predictions that grain boundaries force an imperfect planar-cellular bifurcation.<sup>12</sup>

The experiments we report here were performed with the same seed crystal, which had a grain boundary intersecting the interface 0.3 mm from one sidewall of the

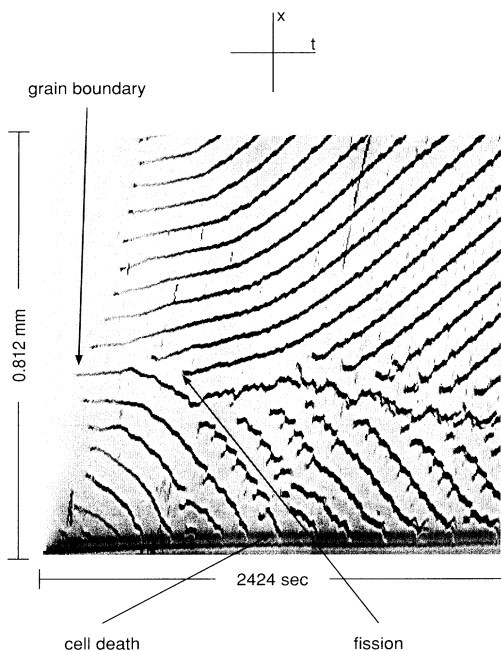


FIG. 1  $x-t$  picture of evolution to the TW state showing the onset of TW states and spatiotemporal dislocations.  $v = 5 \mu\text{m/s}$ .

capillary. After solidification begins at  $v > v_c$ , we first observe a change in the solid-liquid-glass contact angle at the lateral edges of the capillary. The contact angle at  $v = 0$  is about  $60^\circ$  with the liquid wetting the glass. When  $v \neq 0$ , the liquid wets much better and the contact angle becomes immeasurably small. There is a thin layer of liquid between the solid and the glass that can be thought of as an *intrinsic* groove similar to those between cells.

The grain boundary near the middle of the cell opens and a groove of liquid penetrates it. This is the single dark line near the center of Fig. 1. Eventually, the planar interface becomes unstable and ripens into fully developed cells with deep grooves between them.<sup>13</sup> These grooves are the array of dark lines that begin after the grain boundary opens in Fig. 1. The lines originate at the grain boundary; this is the nucleation referred to earlier. When the cellular array is fully established, the cell widths are narrow and fairly regular. The individual cells are also almost exactly symmetric in shape. From onset though, cells begin disappearing at the lateral edges. The first groove out from both sidewalls simply moves closer to the wall until the bracketed cell becomes too narrow to survive and disappears via the well-known *cell-death*<sup>14,15</sup> scenario. In Fig. 1, these are the dark lines ending at the visible lateral edge; the other edge is not visible, but the grooves there suffer the same fate. There is thus one less groove near the edge, and, furthermore, the groove that was originally the second from the

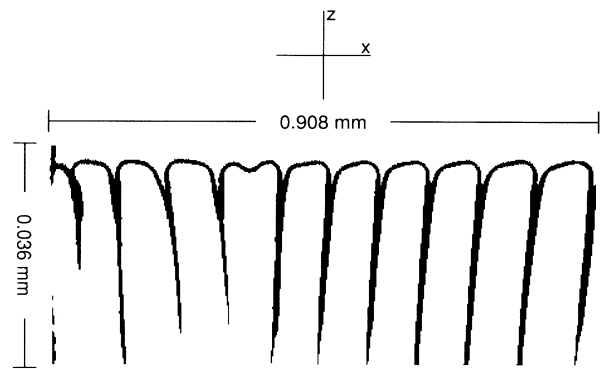


FIG. 2. Binarized photograph of a cellular array. The cells are propagating in the direction they are leaning. Near the center, a cell is undergoing fission. Near the left edge, the cell tip has dropped back somewhat from its neighbors and will soon disappear.  $v = 3 \mu\text{m/s}$ .

edge migrates towards the wall, and the process repeats.

In Fig. 1, although the grooves near the edges are initially parallel to the lateral wall, they begin to tilt towards the walls as cells die there. The effect is to increase the cell widths, especially of those nearer the edges. Eventually a cell becomes too wide to be stable; i.e., its tip becomes so flat that it is subject to the same instability as the original planar interface. The result is a shape instability of an individual cell. This instability can have two outcomes: (a) If the depression of the cell tip is close enough to the center of the cell, “fission”<sup>11</sup> (tip splitting) occurs and two new cells result from one, or (b) if the depression is closer to the cell groove, it temporarily grows but soon dies and moves back along the groove; we have termed this a “mittens” instability.<sup>11</sup> If mittening occurs, the cell width is not adjusted, and eventually fission must happen. In Fig. 1, fission is a new line appearing and remaining while mittening is a new line that disappears into one of its neighbors. In fission, the two new cells, originally narrower than their neighbors, widen to become indistinguishable from them. The cellular array attains a steady state, where the number of cells dying at the edges is balanced by the number being created by fission near the center.

An important feature of the dynamics in Fig. 1 is that it is mediated by cells created near the center traveling to the edges. The grooves have nonzero slope in the  $x-t$  plane which is the signature of a traveling wave (TW). This is the first observation of TW waves in directional solidification where cells have deep grooves as well as the first observation of traveling waves spanning the entire breadth of the pattern.

A feature of this dynamics not discernible from  $x-t$  pictures is the asymmetry of the TW cell tips. Figure 2 is a binarized image of the cellular array. The cells have a dramatic “lean” to one side; one aspect of this lean is a

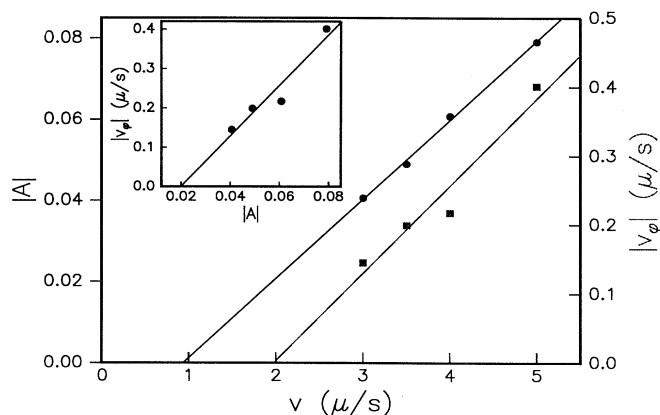


FIG. 3. Phase speed  $v_\phi$  (■) and asymmetry  $A$  (●) as a function of pulling speed  $v$ . The best-fit straight lines are overlaid for both.  $|v_\phi|$  extrapolates to zero at  $v \approx v_c$  and  $|A|$  at  $v \approx v_c/2$ . Inset:  $v_\phi$  as a function of asymmetry.

finite angle between the cell grooves and the pulling direction. Furthermore, the cell grooves on the left are leaning as well as moving to the left; those on the right to the right. Asymmetric cells traveling in the direction dictated by the sign of their asymmetry are also observed in liquid-crystal systems,<sup>1</sup> as well as eutectic mixtures.<sup>3,16</sup>

The phase speed  $v_\phi$  of the TW state is the slope of the lines made by the grooves in the  $x-t$  picture. As seen in Fig. 1,  $v_\phi$  starts at zero, increases (first in the grooves near the edges), and then saturates. Note that there are generally one or two grooves, near the fission site, that have practically zero slope. Figure 3 shows that the saturated  $|v_\phi|$  is linear in the pulling speed and extrapolates to zero at approximately  $v_c$ —the scatter is approximately 20%.

Measuring asymmetry is more subtle. We captured individual frames from the videotape at fixed intervals and binarized them to bring out the solid-liquid interface. Individual cells are digitized using a “left-hand-walker”<sup>17</sup> algorithm so that points on the cell boundary are uniformly distributed, giving the locus  $(x_i, z_i)$  of the solid-side edge of each cell. We then define asymmetry as<sup>18</sup>

$$A \equiv \frac{-\sum_i (x_i - \bar{x})(z_i - \bar{z}) |\sum_i (x_i - \bar{x})(z_i - \bar{z})|}{\sum_i (x_i - \bar{x})^2 \sum_i (z_i - \bar{z})^2}.$$

We have verified that this is proportional to the asymmetry as defined by Coulet, Goldstein, and Gunaratne.<sup>5</sup> Like  $v_\phi$ , the asymmetry starts small, but increases and then saturates in time. Again, similar to  $v_\phi$ , as one goes laterally across the pattern,  $A(x)$  (plotted in Fig. 4) goes through zero, resulting in a kink. Note that the zero of  $A(x)$  is near the fissioning site. The average of  $|A|$  also increases linearly with pulling speed, as shown in Fig. 3.

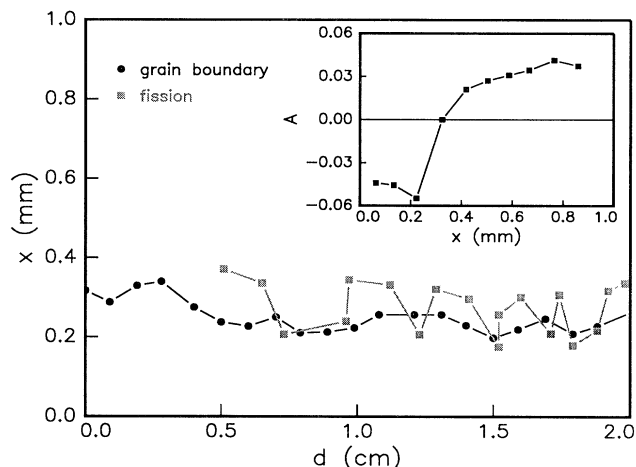


FIG. 4. Strong correlation between distance from lateral edge ( $x$ ), of fissioning site and grain boundary, vs distance pulled ( $d$ ). Inset: The kink  $A(x)$  corresponding to the array in Fig. 2.

However, unlike  $v_\phi$ , it appears to extrapolate to zero at  $v \approx v_c/2$ .

We referred earlier to the relation between crystalline grain boundaries and the *phase source*, or fission site. The grain-boundary position can be observed when the solid is directionally melted because it melts first and a thick line in the solid is seen. Figure 4 shows the strong correlation between its lateral position and the position of the fission site. Further evidence for the crucial importance of grain boundaries is that when they are removed,<sup>10</sup> TW behavior is not observed.

Predictions<sup>5</sup> that phase speed increases linearly with asymmetry have been borne out by our experiments. There is one important difference however; if the predicted linear relationship between these quantities persists to  $|A|=0$ , there is an offset<sup>19</sup> in  $v_\phi$  which is not predicted. Although we observe a strong correlation between asymmetry and TW states, we suggest that the shape distortion of individual cells at higher pulling speeds may be predendritic effects, or equivalently, related to the oscillatory instability predicted by Karma and Pelcé.<sup>20</sup> Indeed, Fig. 5 is a magnification of one section of an  $x-t$  plot. The grooves can be seen to be “staircasing” in concert with each other, indicative of a coherent, periodic, mitten instability of individual cells. Also, faintly discernible are lines periodically crossing the cells joining adjacent steps; these lines are mitten instabilities in the viewing direction. The power spectrum of a cell root digitized from this image reveals a resolution-limited peak at a period of 40.3 s, which is  $D/v^2$ , the diffusion time.<sup>21</sup>

In conclusion, we have demonstrated the existence of traveling waves and asymmetric cells in deep-groove directional solidification and measured both the phase

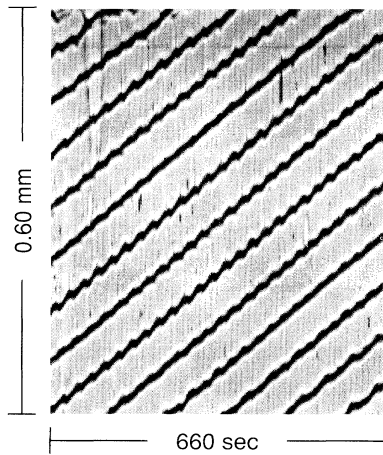


FIG. 5. Magnified  $x-t$  image showing the coherent (over at least seven cells), periodic, wavy instability observed at  $v=5 \mu\text{m/s}$ . The period is approximately  $D/v^2$ , where  $D$  is the impurity diffusion constant.

speed and asymmetry. These measurements exhibit qualitative agreement with existing theory. The asymmetry extends over the entire pattern except for a localized kink. We observe both sinks and sources of phase and have identified the former with crystalline grain boundaries and the latter with a small liquid-solid-glass contact angle. The shape asymmetry may be related to predendritic, coherent, oscillation effects.

We thank R. Goldstein, W. van Saarloos, P. Kolodner, G. Faivre, C. Caroli, and D. Grier for insightful discussions. J.T.G. acknowledges support from the Natural Sciences and Engineering Research Council (Canada).

<sup>1</sup>A. Simon, J. Bechhoefer, and A. Libchaber, *Phys. Rev. Lett.* **61**, 2574 (1988).

<sup>2</sup>F. Melo and P. Oswald, *Phys. Rev. Lett.* **64**, 1381 (1990).

<sup>3</sup>G. Faivre, S. de Cheveigné, C. Guthmann, and P. Kurowski, *Europhys. Lett.* **9**, 779 (1989).

<sup>4</sup>M. Rabaud, S. Michalland, and Y. Couder, *Phys. Rev. Lett.* **64**, 184 (1990).

<sup>5</sup>P. Coulet, R. E. Goldstein, and G. H. Gunaratne, *Phys.*

*Rev. Lett.* **63**, 1954 (1989); R. E. Goldstein, G. H. Gunaratne, and L. Gil, *Phys. Rev. A* **41**, 5731 (1990); R. E. Goldstein, G. H. Gunaratne, L. Gil, and P. Coulet (to be published).

<sup>6</sup>H. Levine, W. J. Rappel, and H. Riecke (to be published).

<sup>7</sup>In Ref. 2 it is not clear what the extent of the asymmetric inclusion is.

<sup>8</sup>A subcritical bifurcation was proposed because previously observed asymmetric states have been localized inclusions.

<sup>9</sup>This is determined by differential scanning calorimetry and agrees well with that obtained using the observed value of  $I_T$  predicted using the constitutional supercooling criterion; see J. S. Langer, *Rev. Mod. Phys.* **52**, 1 (1980).

<sup>10</sup>P. E. Cladis, P. L. Finn, and J. T. Gleeson, in *Nonlinear Evolution of Spatio-Temporal Structures in Dissipative Continuous Systems*, edited by F. Busse and L. Kramer (Plenum, New York, 1990).

<sup>11</sup>P. E. Cladis, J. T. Gleeson, and P. L. Finn, in *Defects, Patterns and Instabilities*, edited by D. Walgraef and N. Ghoniem (Kluwer, Dordrecht, 1990).

<sup>12</sup>L. H. Ungar and R. A. Brown, *Phys. Rev. B* **30**, 3993 (1984).

<sup>13</sup>This is the Mullins-Sekerka instability; W. W. Mullins and R. F. Sekerka, *J. Appl. Phys.* **35**, 444 (1964).

<sup>14</sup>V. Seetharaman, M. A. Eshelman, and R. Trivedi, *Acta Metall.* **36**, 1175 (1988).

<sup>15</sup>S. de Cheveigné, C. Guthmann, and M. M. Lebrun, *J. Phys. (Paris)* **47**, 2095 (1986).

<sup>16</sup>In eutectic solidification, tilt waves must have this asymmetry to conserve the number of lamellae; G. Faivre (private communication).

<sup>17</sup>The inside (solid-side) edge is found in the same way a maze may be solved by searching the image such that a point on the edge is always to the immediate left of the current point.

<sup>18</sup>Consider a set of uniform point masses at  $(x_i, z_i)$ —the numerator is the square (with sign retained) of the product of inertia of this set while the denominator contains the two moments of inertia.

<sup>19</sup>Note, however, that  $v_\phi=0$  when  $v=v_c$  so (in this system) no TW state implies a stable planar interface. We have observed that front propagation speed also can be nonzero when  $v \approx v_c$ ; P. E. Cladis, J. T. Gleeson, and P. L. Finn (to be published).

<sup>20</sup>A. Karma and P. Pelcé, *Phys. Rev. A* **39**, 4162 (1989), predicted a symmetric coherent oscillatory instability. Although the oscillations we observe are not symmetric on individual cells, they do exhibit long-range coherence.

<sup>21</sup> $D$  is the liquid impurity  $\approx 10^{-5} \text{ cm}^2/\text{s}$ ; see M. A. Chopra, M. E. Glicksman, and N. B. Singh, *J. Cryst. Growth* **92**, 543 (1988).

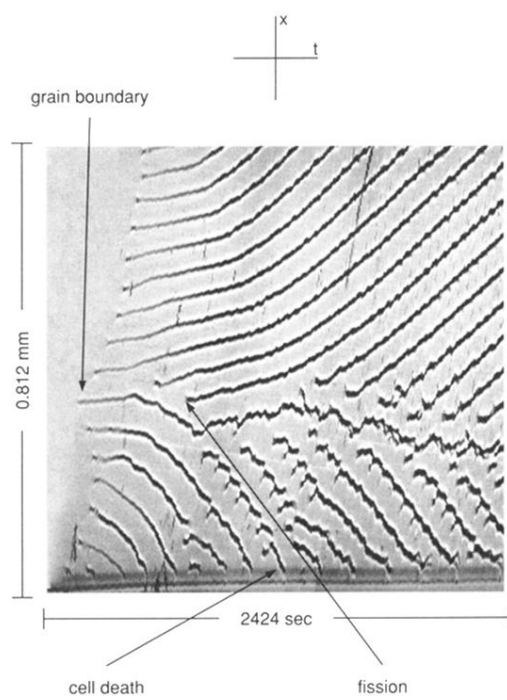


FIG. 1  $x-t$  picture of evolution to the TW state showing the onset of TW states and spatiotemporal dislocations.  $v = 5 \mu\text{m/s}$ .

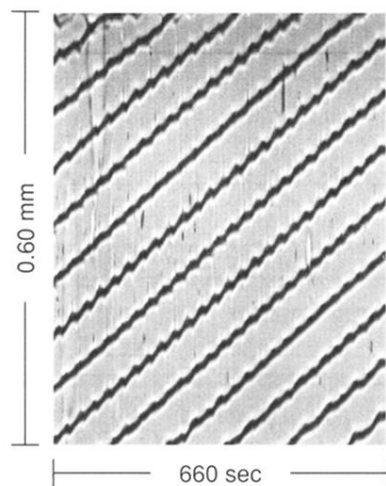


FIG. 5. Magnified  $x-t$  image showing the coherent (over at least seven cells), periodic, mittern instability observed at  $v=5 \mu\text{m/s}$ . The period is approximately  $D/v^2$ , where  $D$  is the impurity diffusion constant.